

Chapter 2

Some Aspects on Global Analysis of Discrete Time Dynamical Systems

Anastasiia Panchuk

Abstract Dynamical systems theory distinguishes two types of bifurcations: those which can be studied in a small neighborhood of an invariant set (local) and those which cannot (global). In contrast to local bifurcations, global ones cannot be investigated by a Taylor expansion, neither they are detected by purely performing stability analysis of periodic points. Global bifurcations often occur when larger invariant sets of the system collide with each other or with other fixed points/cycles. This chapter focuses on several aspects of global bifurcation analysis of discrete time dynamical systems, covering homoclinic bifurcations as well as inner and boundary crises of attracting sets.

2.1 Introduction

Dynamical systems theory is mainly interested in asymptotic behavior of orbits depending on the initial state and how this behavior may change when varying system parameters. The important phenomenon is a bifurcation when the changes occurring in the state space cannot be obtained via a smooth transformations (the orbits before and after the bifurcation are not topologically conjugated). Two types of structural changes are distinguished: local and global ones. Local bifurcations are those which can be examined locally via an approximation of the map in a small neighborhood of some fixed point or cycle. Global bifurcations often occur when larger invariant sets of the system collide with each other or with other fixed points/cycles. Such a global bifurcation cannot be investigated by a Taylor expansion and cannot be detected by purely performing stability analysis of a periodic point. To understand what happens with orbits of the system in this case, one has to take into account global properties of the map (see [17, 27, 34] to cite a few).

A. Panchuk (✉)
Institute of Mathematics, National Academy of Sciences of Ukraine,
Tereshchenkivska str. 3, Kiev 01601, Ukraine
e-mail: anastasiia.panchuk@gmail.com

© Springer International Publishing Switzerland 2016
G.I. Bischi et al. (eds.), *Qualitative Theory of Dynamical Systems, Tools and Applications for Economic Modelling*, Springer Proceedings in Complexity,
DOI 10.1007/978-3-319-33276-5_2

Among common examples of global phenomena, one may list contact bifurcations, homoclinic bifurcations, and crises. Contact bifurcations are characterized by structural changes of basin and its boundary (for example, when a connected basin transforms to a nonconnected one or basin boundary becomes fractal). These bifurcations are only possible in noninvertible maps and occur due to tangencies between basin boundaries and critical curves (for more detail see, e.g., [5, 12, 25] and references therein).

Homoclinic bifurcations entail changing shape of invariant sets and are associated with appearance of homoclinic points (and, consequently, orbits) when the stable and unstable sets of a periodic point have a contact (see, for instance, [6, 8, 10]). This often allows to show strictly existence of an invariant set on which dynamics is chaotic. It can also happen, that the stable set of one periodic point intersects with the unstable set of another periodic point in which case the intersection point (and its orbit) is called heteroclinic. Homoclinic/heteroclinic orbits may also appear in a sequence of bifurcations leading to creation of closed invariant curves (see, e.g., [1, 2]).

Bifurcations called crises are related to sudden transformations of chaotic attractors and encountered in both invertible and noninvertible maps alike homoclinic bifurcations. Such swift changes occur due to a contact between a chaotic attractor and an unstable periodic orbit (or, equivalently, its stable set). Starting from [16], three types of crisis are usually distinguished: a boundary crisis at which the attractor is destroyed, an interior crisis accompanied with abrupt increase in size of the attractor, and merging crisis where several chaotic attractors collide simultaneously with an orbit on the separating basin boundary.

In the current chapter we point out several aspects related to global analysis of discrete time dynamical systems, covering homoclinic bifurcations as well as interior and boundary crises.

2.2 Preliminaries

In this section we introduce general concepts and notations used throughout the chapter.

Let us consider a smooth (or piecewise smooth) function $T : X \rightarrow X$, $X \subseteq \mathbb{R}^n$, $T = (T_1, \dots, T_n)$, which can be invertible or noninvertible. Here $n \in \mathbb{Z}^+$ with \mathbb{Z}^+ denoting the set of all positive integer numbers. Recall that:

- For an arbitrary point $\mathbf{x} \in X$ the value $T(\mathbf{x})$ is called a *rank-1 image* of \mathbf{x} or simply an *image* of \mathbf{x} .
- From definition of T it follows that $T(\mathbf{x}) \in X$. Hence, we may define $T(T(\mathbf{x}))$, $T(T(T(\mathbf{x})))$, and so on. For shortness, the composition of t consecutive applications of the function T to the vector \mathbf{x} is abbreviated as $T^t(\mathbf{x})$, i.e.,

$$\underbrace{T(T(\dots T(\mathbf{x}) \dots))}_t \equiv \underbrace{T \circ T \dots \circ T(\mathbf{x})}_t \stackrel{\text{def}}{=} T^t(\mathbf{x}).$$

- For any $\mathbf{x} \in X$ the value $T^t(\mathbf{x})$, $t \in \mathbb{Z}^+$, is called a *rank- t image* of \mathbf{x} .
- For an arbitrary $\mathbf{x} \in X$ the value $\mathbf{y} \in X$ such that $T^t(\mathbf{y}) = \mathbf{x}$, $t \in \mathbb{Z}^+$, is called a *rank- t preimage* of \mathbf{x} . The set of all rank- t preimages is denoted as $T^{-t}(\mathbf{x})$. For shortness, we refer to a rank-1 preimage of \mathbf{x} simply as a *preimage* of \mathbf{x} .

It is important to mention, that for an arbitrary $\mathbf{x} \in X$ its rank- t image, $t \in \mathbb{Z}^+$, exists and is unique. This is not necessarily true for preimages of \mathbf{x} that may be multiple ($T^{-t}(\mathbf{x})$ has more than one element) or missing ($T^{-t}(\mathbf{x}) = \emptyset$), in case where T is noninvertible.

For avoiding confusion we emphasize that whenever the symbol $T^{-1}(\mathbf{x})$ is used, it is meant to denote the set of *all preimages* of a certain point \mathbf{x} . However, writing simply T^{-1} (without \mathbf{x}) we have in mind an *inverse function* of T . In case where T is a bijection (a one-to-one and onto), each $\mathbf{x} \in X$ has exactly one (rank-1) preimage (the set $T^{-1}(\mathbf{x})$ consists of a single point). Then, the function T is called *invertible* and the inverse function T^{-1} can be uniquely defined. On the other hand, if T is not bijective, then it is *noninvertible* and the set $T^{-1}(\mathbf{x})$ may consist of more than one value or be empty depending on \mathbf{x} (hence, the inverse function T^{-1} is either not defined uniquely or not defined for some $\mathbf{x} \in X$).

Example 2.1 Consider the function $T_\mu = \mu\sqrt{x}$, $0 < \mu \leq 1$, with $X = [0, 1]$. It is clear that $T_\mu(X) = [0, \mu]$. Consequently, for $\mu < 1$ the points $\bar{x} > \mu$ do not have preimages, that is, $T_\mu^{-1}(\bar{x}) = \emptyset$ and the inverse function T_μ^{-1} is only defined for $x \in [0, \mu]$. Nevertheless, the dynamical system related to T_μ do not produce complex behavior since T_μ is monotonically increasing.

Example 2.2 Consider the function $T = 4x(1 - x)$ with $X = [0, 1]$. The image of X is $T(X) = [0, 1] = X$, but every $x \in X$, except for $\bar{x} = 1$, has two preimages $y_{\mathcal{L}} < 0.5$ and $y_{\mathcal{R}} > 0.5$. The inverse function T^{-1} can not be uniquely defined, though one may define two distinct inverse functions of T . That is, $T_{\mathcal{L}}^{-1} : [0, 1] \rightarrow [0, 0.5]$ and $T_{\mathcal{R}}^{-1} : [0, 1] \rightarrow [0.5, 1]$ with obvious equality $T_{\mathcal{L}}^{-1}(1) = T_{\mathcal{R}}^{-1}(1) = 0.5$.

Let us consider now a *discrete* (or discrete time) dynamical system (DDS for short) represented by the iterative relation

$$\mathbf{x}_{t+1} = T(\mathbf{x}_t) \quad t \in \mathbb{Z}^*, \tag{2.1}$$

where $\mathbb{Z}^* = \mathbb{Z}^+ \cup \{0\}$ is a set of all non-negative integers, or, in equivalent notation,

$$\mathbf{x}' = T(\mathbf{x}), \tag{2.1'}$$

where \mathbf{x}' denotes the next iterate under T (image of x). Having in mind the evolutionary process (2.1) the function T is often referred to as a *map* or a *mapping*. The set X then serves as the *state space*, while an n -dimensional real vector $\mathbf{x} = (x_1, \dots, x_n) \in X$ is the *state variable*.

For every initial state $\mathbf{x}_0 \in X$ of the system (2.1) or (2.1') at the time $t = 0$, the sequence of successive images of \mathbf{x}_0 constitutes a *discrete trajectory* or an *orbit*:

$$\mathcal{O}(\mathbf{x}_0) = \{T^t(\mathbf{x}_0)\}_{t=0}^{\infty} = \{\mathbf{x}_0, \mathbf{x}_1, \dots, \mathbf{x}_t, \dots\}. \quad (2.2)$$

Here T^0 denotes the identity function (map), namely, $T^0(\mathbf{x}) = \mathbf{x}$ for any $\mathbf{x} \in X$.

The main task in studying a dynamical system (2.1) is to understand the asymptotic behavior of its orbits depending on the initial condition \mathbf{x}_0 and how this develops with changing parameters. For instance, an orbit can “stuck” at some invariant set or diverge to infinity, and this behavior may be different depending on \mathbf{x}_0 . It may also happen that an orbit diverges from some invariant set, but then comes back to it again due to existence of a homoclinic orbit.

Recall that a set $A \subset X$ is called *invariant* under T or *T-invariant* if it is mapped onto itself $T(A) = A$. The two simplest kinds of invariant sets (and, hence, the simplest asymptotic behavior of orbits of (2.1)) are

- a *fixed point* \mathbf{x}^* such that $T(\mathbf{x}^*) = \mathbf{x}^*$, and
- a *k-cycle*, $\mathcal{C}_k = \{\mathbf{x}_1^*, \dots, \mathbf{x}_k^*\}$ such that $\mathbf{x}_{i+1}^* = T(\mathbf{x}_i^*)$, $\mathbf{x}_1^* = T(\mathbf{x}_k^*)$.

However, the structure of an invariant set A may be much more complex than just a point or a finite set of points, and this fact led to introducing such terms as *strange attractor* [15, 29] and *chaotic attractor* [9, 21]. There exist many possible definitions of chaos in dynamical systems theory, some of them being stronger than the others. Here we follow the definition given by Devaney [7].

Definition 2.1 Consider a map $T : X \rightarrow X$ and let a set $A \subset X$ be invariant under T . The restriction $T|_A : A \rightarrow A$ is called *chaotic* on A if

- (i) there exist infinitely many periodic orbits dense in A ,
- (ii) $T|_A$ is *topologically transitive*, that is, for any pair of open sets $U, V \subset A$ there exists $t \in \mathbb{Z}^+$ such that $T^t(U) \cap V \neq \emptyset$.

The set A is also often said to be *chaotic*.

To be precise, in his definition Devaney also includes the third property that $T|_A$ has sensitive dependence on initial conditions,¹ although this property can be derived from the other two (see, e.g., [4]). The chaos of the described type is also called topological chaos, that is having positive topological entropy.

It is worth to mention that condition (ii) is often replaced by

- (ii') there exists an aperiodic orbit dense in A .

Conditions (ii') and (ii) are not connected in general, though under additional requirements on A they become equivalent. Namely, if A has no isolated points then (ii')

¹The map $T : X \rightarrow X$ is said to have *sensitive dependence on initial conditions* if there exists $\delta > 0$ such that for any $\mathbf{x} \in X$ and any neighborhood $U(\mathbf{x})$ there exist $\mathbf{y} \in U(\mathbf{x})$ and $t \geq 0$ such that $|T^t(\mathbf{x}) - T^t(\mathbf{y})| > \delta$.

implies (ii). The opposite is true if A contains a countable dense subset and is of second category² (see, e.g., [32]).

One might expect that chaotic behavior is more natural for DDS with dimension $n \geq 2$, however, already one-dimensional *noninvertible* maps can show non-regular dynamics of this kind. One of the most known examples is a family of quadratic maps such as logistic map [31] or conjugated to it Myrberg map [26].

In the next sections we describe a couple of phenomena due to which a chaotic attractor may appear or be reshaped. For that we first introduce such important concepts as stable and unstable sets of a fixed point or a cycle.

2.3 Stable and Unstable Sets

The stable and the unstable set of a fixed point or a cycle are important concepts for studying behavior of a dynamical system globally. They are related to boundaries of basins of attraction, saddle-connections and birth of closed invariant curves, homoclinic tangles, appearance and modification of chaotic attractors. Classically, these notions are defined for maps of dimension greater than one, which are characterized by possibility of both expansion and contraction in the same invariant set. However, an extension of the idea to a class of one-dimensional noninvertible maps was given already in 1969 by Sharkovsky [30] and then developed in [22, 25] among the others.

2.3.1 Stable Manifold Theorem

Let consider a DDS (2.1) and denote

$$DT(\mathbf{x}) = \begin{pmatrix} \frac{\partial T_1(\mathbf{x})}{\partial x_1} & \cdots & \frac{\partial T_1(\mathbf{x})}{\partial x_n} \\ \cdots & \cdots & \cdots \\ \frac{\partial T_n(\mathbf{x})}{\partial x_1} & \cdots & \frac{\partial T_n(\mathbf{x})}{\partial x_n} \end{pmatrix}$$

the Jacobian matrix of the map T at the point \mathbf{x} . And let $\lambda_i = \lambda_i(\mathbf{x})$, $1 \leq i \leq n$, be the eigenvalues of $DT(\mathbf{x})$.

Definition 2.2 A fixed point \mathbf{x}^* of the map T is called *hyperbolic* if $DT(\mathbf{x}^*)$ has no eigenvalues on the unit circle, that is, $|\lambda_i(\mathbf{x}^*)| \neq 1$, $1 \leq i \leq n$.

For sake of shortness, we drop the symbol (\mathbf{x}^*) in notation of eigenvalues whenever it is clear which point is meant. If all λ_i , $1 \leq i \leq n$, of $DT(\mathbf{x}^*)$ are inside the unit

²A subset A of a topological space X is said to be of *second category* in X if A cannot be written as the countable union of subsets which are nowhere dense in X .

circle ($|\lambda_i| < 1$), then \mathbf{x}^* is *attracting* (more precisely, asymptotically stable), while in case when all $|\lambda_i| > 1$, the point \mathbf{x}^* is called *expanding*. In the intermediate case, when some of eigenvalues of \mathbf{x}^* are inside the unit circle and others are outside it, the point \mathbf{x}^* is referred to as *saddle* or *unstable*.³ Clearly, for a one-dimensional map the concepts of expanding and unstable fixed points are equivalent.

Let rearrange the eigenvalues of $DT(\mathbf{x}^*)$ so that $|\lambda_i| < 1$ for $1 \leq i \leq i_0$ and $|\lambda_i| > 1$ for $i_0 < i \leq n$ and consider the sets of related eigenvectors. Let $E^s(\mathbf{x}^*)$ denote a subspace of dimension i_0 spanned on the eigenvectors $\{\mathbf{v}_1, \dots, \mathbf{v}_{i_0}\}$ corresponding to eigenvalues being inside the unit circle. Then $E^s(\mathbf{x}^*)$ is called a *stable eigenspace* of \mathbf{x}^* . Similarly, the eigenvectors $\{\mathbf{v}_{i_0+1}, \dots, \mathbf{v}_n\}$ corresponding to eigenvalues outside the unit circle define an *unstable eigenspace* $E^u(\mathbf{x}^*)$ (whose dimension is clearly $n - i_0$).

Example 2.3 Let consider a linear mapping $T_{\text{lin}} : \mathbb{R}^2 \rightarrow \mathbb{R}^2$,

$$T_{\text{lin}} : \begin{cases} x'_1 = 2x_1 + x_2, \\ x'_2 = x_1 + x_2. \end{cases}$$

It obviously has a fixed point $\mathbf{x}^* = (0, 0)$ with Jacobian

$$DT_{\text{lin}}(0, 0) = \begin{pmatrix} 2 & 1 \\ 1 & 1 \end{pmatrix}. \quad (2.3)$$

The eigenvalues of $DT_{\text{lin}}(0, 0)$ are $\lambda_1 = (3 - \sqrt{5})/2$, $\lambda_2 = (3 + \sqrt{5})/2$ with the corresponding eigenvectors $\mathbf{v}_i = (1/(\lambda_i - 2), 1)$, $i = 1, 2$. Since $\lambda_1 < 1$, the stable eigenspace is

$$E^s(0, 0) = \{\alpha \mathbf{v}_1 \mid \alpha \in \mathbb{R}\}, \quad (2.4)$$

that is, the line defined by the vector \mathbf{v}_1 . Similarly, the vector \mathbf{v}_2 gives the unstable eigenspace

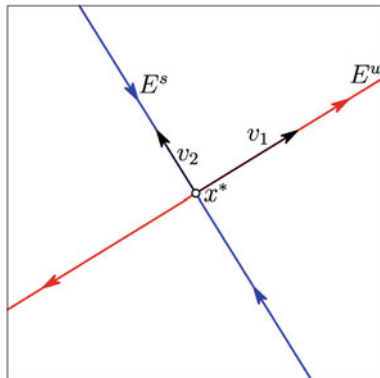
$$E^u(0, 0) = \{\alpha \mathbf{v}_2 \mid \alpha \in \mathbb{R}\}, \quad (2.5)$$

being the line orthogonal to $E^s(0, 0)$ (see Fig. 2.1).

Now, we directly come to introducing the notions of stable and unstable sets. First, the classical case is considered where the mapping T is a diffeomorphism, that is, a smooth bijective function. Then, modified versions of the definitions are given so that to cover the case of noninvertible and/or piecewise smooth maps.

³Some authors use also the term *repelling* in this case, though it might be confusing since there is more strict definition of a repelling set.

Fig. 2.1 Stable E^s and unstable E^u eigenspaces of the saddle fixed point \mathbf{x}^*



2.3.1.1 Diffeomorphisms: Stable and Unstable Manifolds

Definition 2.3 Let the mapping T be a diffeomorphism, and let \mathbf{x}^* be a hyperbolic fixed point of the system (2.1). The sets

$$W^s(\mathbf{x}^*) = \{\mathbf{y} \in X : \lim_{t \rightarrow \infty} T^t(\mathbf{y}) = \mathbf{x}^*\}, \quad (2.6)$$

$$W^u(\mathbf{x}^*) = \{\mathbf{y} \in X : \lim_{t \rightarrow \infty} T^{-t}(\mathbf{y}) = \mathbf{x}^*\} \quad (2.7)$$

are called the *stable* and the *unstable set* of \mathbf{x}^* , respectively.

Note that if \mathbf{x}^* is an expanding fixed point, then its stable set is empty, while its unstable set is some n -dimensional area (the shape of this area depends on presence of other invariant sets of the system). On the contrary, if \mathbf{x}^* is an asymptotically stable fixed point, then its unstable set is empty, while its stable set is just its basin of attraction.

The Stable Manifold Theorem (see, e.g., [3, 34]) guarantees that $W^s(\mathbf{x}^*)$ and $W^u(\mathbf{x}^*)$ exist and are manifolds of the same smoothness as T .

Theorem 2.1 (Stable Manifold Theorem) *Let T be a diffeomorphism and \mathbf{x}^* be a hyperbolic fixed point of the DDS (2.1). Then $W^s(\mathbf{x}^*)$ is as smooth as T manifold and the stable eigenspace $E^s(\mathbf{x}^*)$ is tangent to $W^s(\mathbf{x}^*)$ at the point \mathbf{x}^* .*

Applying Theorem 2.1 to the inverse T^{-1} , the same can be stated about the unstable set $W^u(\mathbf{x}^*)$, that is, $W^u(\mathbf{x}^*)$ is as smooth as T manifold and $E^u(\mathbf{x}^*)$ is its tangent space at \mathbf{x}^* . For sake of shortness, we drop the symbol (\mathbf{x}^*) in notation of eigenspaces and stable/unstable manifolds whenever it is clear which point is meant.

Example 2.4 In case of linear mapping T (such as the one in Example 2.3), the stable/unstable manifold W^s/W^u of the fixed point $\mathbf{x}^* = (0, 0)$ coincides with the stable/unstable eigenspace E^s/E^u . We demonstrate this for the stable manifold, and the unstable one is treated likewise. First, we show that E^s is invariant under

T . Let $\mathbf{x} \in E^s$ which means that $\mathbf{x} = \alpha \mathbf{v}_1$ with a certain $\alpha \in \mathbb{R}$. Then $T(\mathbf{x}) = T(\alpha \mathbf{v}_1) = \alpha \lambda_1 \mathbf{v}_1$ and, hence, $T(\mathbf{x}) \in E^s$. And vice versa: consider $T(\mathbf{x}) \in E^s$, that is, $T(\mathbf{x}) = \alpha \mathbf{v}_1$, which is equivalent to $T(\lambda_1 \mathbf{x} / \alpha) = \lambda_1 \mathbf{v}_1$. The latter clearly implies $\mathbf{x} = \alpha \mathbf{v}_1 / \lambda_1 \in E^s$.

It remains to verify that for any $\mathbf{y} \in E^s$ there holds $\lim_{t \rightarrow \infty} T^t(\mathbf{y}) = \mathbf{x}^*$. Indeed, $T^t(\mathbf{y}) = \alpha \lambda_1^t \mathbf{v}_1$, $\alpha \in \mathbb{R}$. Obviously, $\lim_{t \rightarrow \infty} \|T^t(\mathbf{y})\| = 0$ since $|\lambda_1| < 1$.

2.3.1.2 Noninvertible Maps: Stable and Unstable Sets

Now, we consider the more general case where T is not a diffeomorphism, namely, T may be noninvertible and/or piecewise smooth. The definition (2.6) for the stable set $W^s(\mathbf{x}^*)$ remains unchanged, but the expression (2.7) for the unstable set $W^u(\mathbf{x}^*)$ has to be modified with taking into account that the points can have more than one preimage.

Definition 2.4 Let T be a continuous piecewise smooth map and consider a hyperbolic fixed point \mathbf{x}^* of the DDS (2.1). The locus of points having a sequence of preimages that tends towards \mathbf{x}^* , that is,

$$W^u(\mathbf{x}^*) = \left\{ \mathbf{y} \in X : \exists \{\mathbf{z}_t\}_{t=0}^{\infty}, \mathbf{z}_0 = \mathbf{y}, T(\mathbf{z}_{t+1}) = \mathbf{z}_t \text{ such that } \lim_{t \rightarrow \infty} \mathbf{z}_t = \mathbf{x}^* \right\}, \quad (2.8)$$

is called the *unstable set* of \mathbf{x}^* .

Note that in this definition *not all* preimages of \mathbf{y} tend towards \mathbf{x}^* , but *there exists* an infinite sequence of preimages of \mathbf{y} having \mathbf{x}^* as a limit point. Moreover, in case of a noninvertible T , the stable set of an expanding fixed point may be nonempty (in contrast to invertible maps). More precisely, it consists of all preimages of this fixed point. Similarly, the unstable set of an asymptotically stable fixed point \mathbf{x}^* may be nonempty.

Clearly, in case of noninvertible or non-smooth T , the Stable Manifold Theorem (Theorem 2.1) cannot be applied directly. We additionally require that (i) the point \mathbf{x}^* is not *degenerate*, that is, $\det DT(\mathbf{x}^*) \neq 0$ (the Jacobian have no zero eigenvalues), and (ii) T is smooth at \mathbf{x}^* . If these two conditions are satisfied there exists a neighborhood $U(\mathbf{x}^*)$ such that $T|_{U(\mathbf{x}^*)}$ is a diffeomorphism. Hence, Theorem 2.1 guarantees existence of *local stable* $W_{\text{loc}}^s(\mathbf{x}^*) \subset U(\mathbf{x}^*)$ and *local unstable* $W_{\text{loc}}^u(\mathbf{x}^*) \subset U(\mathbf{x}^*)$ manifolds, which are tangent at \mathbf{x}^* to the stable and unstable eigenspaces $E^s(\mathbf{x}^*)$ and $E^u(\mathbf{x}^*)$, respectively. Then the *global stable* and *global unstable sets* can be alternatively defined as

$$W^s(\mathbf{x}^*) = \bigcup_{t=0}^{\infty} T^{-t}(W_{\text{loc}}^s(\mathbf{x}^*)), \quad (2.9)$$

$$W^u(\mathbf{x}^*) = \bigcup_{t=0}^{\infty} T^t(W_{\text{loc}}^u(\mathbf{x}^*)). \quad (2.10)$$

Example 2.5 Let consider a nonlinear function $T_{\text{nonlin}} : \mathbb{R}^2 \rightarrow \mathbb{R}^2$,

$$T_{\text{nonlin}} : \begin{cases} x'_1 = 2x_1 + x_2, \\ x'_2 = x_1 - x_1^2 + x_2, \end{cases}$$

which is clearly noninvertible. It has a fixed point $\mathbf{x}^* = (0, 0)$ with the same Jacobian (2.3) as in Example 2.3. Consequently, the stable E^s and unstable E^u eigenspaces of \mathbf{x}^* are given by (2.4) and (2.5), respectively. The stable W^s and unstable W^u sets of \mathbf{x}^* cannot be derived in analytic form, but one may approximate them numerically. In Fig. 2.2 the sets W^s and W^u together with E^s and E^u are shown.

In general, stable and unstable sets of a fixed point \mathbf{x}^* have the following properties (see, e.g., [25]):

1. W^s is backward invariant, but not necessarily (forward) invariant (mapped only into itself), that is,

$$\begin{aligned} T^{-1}(W^s) &= W^s, \\ T(W^s) &\subseteq W^s. \end{aligned}$$

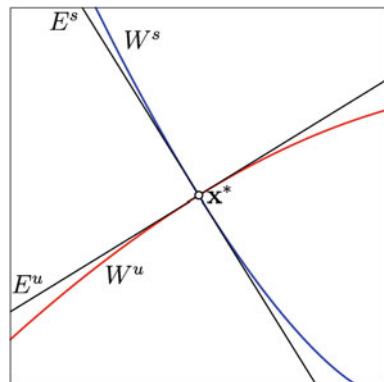
2. W^u is invariant, but not necessarily backward invariant:

$$\begin{aligned} T(W^u) &= W^u, \\ T^{-1}(W^u) &\supseteq W^u. \end{aligned}$$

3. Both W^s and W^u are not necessarily manifolds and may have self intersections.
4. When T is continuous, the set W^u is connected, while W^s may consist of disjoint connected components.

The notions of stable and unstable sets can be generalized for a k -cycle $\mathcal{C}_k = \{\mathbf{x}_1^*, \dots, \mathbf{x}_k^*\}$ by considering T^k , for which every point \mathbf{x}_i^* is a fixed point. Then under

Fig. 2.2 Stable W^s and unstable W^u sets of the saddle fixed point \mathbf{x}^* together with related eigenspaces



the stable (unstable) set of \mathcal{C}_k one mean the union of all stable (unstable) sets $W^s(\mathbf{x}_i^*)$ ($W^u(\mathbf{x}_i^*)$).

As one can see, the stable and unstable sets are not defined only in a neighborhood of a fixed point (or a cycle), but in the larger area of the state space and may even extend to infinity. Due to this reason, they often play an important role when studying global properties of the map T . In particular,

1. stable sets of saddle points or cycles may define boundaries of basins of attraction;
2. stable sets of saddle cycles may establish saddle-connections (homoclinic/heteroclinic loops) inducing creation of closed invariant curves.
3. stable and unstable sets may attain a very complex configuration generating a homoclinic tangle, which causes then appearance of an invariant chaotic set;
4. contact of the stable set of a saddle periodic point with another invariant set may lead to a crisis bifurcation.

The situation (1) is briefly explained immediately below by using a simple example. The phenomenon (3) is described in detail in Sect. 2.4. Interior and boundary crises (4) are considered in Sect. 2.5. The item (2) is beyond the scopes of the current chapter, and the reader is referred to [1, 2] and references therein.

2.3.2 Stable Sets of Saddle Points and Basins

Let us consider a two-parametric family $H_{a,b} : \mathbb{R}^2 \rightarrow \mathbb{R}^2$ such that

$$H_{a,b} : \begin{pmatrix} x \\ y \end{pmatrix} \rightarrow \begin{pmatrix} a - by - x^2 \\ x \end{pmatrix}. \quad (2.11)$$

The map (2.11) is called Hénon map⁴ (see, e.g., [7, 18]). Note that $H_{a,b}$ has only one nonlinear term, so that, it is indeed one of the simplest nonlinear maps in higher dimensions.

It is easy to calculate the Jacobi matrix of $H_{a,b}$:

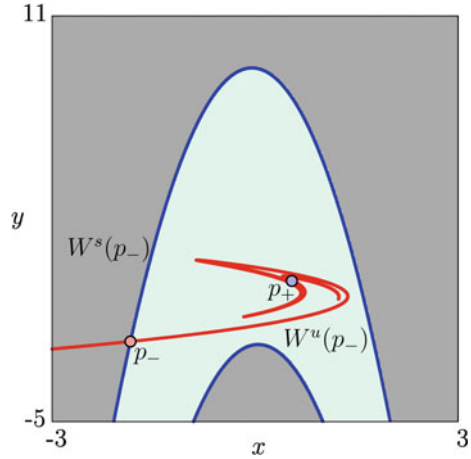
$$DH_{a,b} = \begin{pmatrix} -2x & -b \\ 1 & 0 \end{pmatrix},$$

whose determinant is $\det DH_{a,b} = b$. Clearly, if $b \neq 0$, then the mapping (2.11) is invertible, and its inverse is given as

$$H_{a,b}^{-1} : \begin{pmatrix} x \\ y \end{pmatrix} \rightarrow \begin{pmatrix} x \\ -\frac{a}{b} - \frac{y}{b} + \frac{x^2}{b} \end{pmatrix}. \quad (2.12)$$

⁴In the original paper of M. Hénon this map is written in slightly different form, namely, $\tilde{H}_{a,b} : (x, y) \rightarrow (1 + y - ax^2, bx)$, but topological conjugacy between $\tilde{H}_{a,b}$ and $H_{a,b}$ can be easily shown.

Fig. 2.3 Phase space of the Hénon map $H_{a,b}$ with $a = 1$, $b = 0.3$. The basin of the attracting fixed point \mathbf{p}_+ is confined by the stable set of the saddle \mathbf{p}_+ (namely, it is the area between the two parabola-shaped curves). Orbits starting in the dark-gray region diverge to infinity



It can be shown that for any $a \in \mathbb{R}, b \in \mathbb{R} \setminus \{0\}$ the map $H_{a,b}$ is topologically conjugate to $H_{A,B}^{-1}$ with $A = -a/b^2, B = -1/b$. Hence, it is enough to consider $|b| \leq 1$.

Note that in case $b = 0$, the function $H_{a,0}$ is noninvertible and maps the entire plane onto a parabola $P = \{(x, y) : x = a - y^2\}$, which implies topological conjugacy between the restriction $H_{a,0}|_P$ and the Myrberg map [26].

We set $a = 1, b = 0.3$, for which $H_{1,0.3}$ has two fixed points: a saddle $\mathbf{p}_- = (x_-, x_-)$ and a sink $\mathbf{p}_+ = (x_+, x_+)$. In Fig. 2.3 a part of the phase space is shown. The basin of attraction $\mathcal{B}(\mathbf{p}_+)$ of the sink \mathbf{p}_+ is confined by the stable set $W^s(\mathbf{p}_-)$ (a part of this stable set appears in Fig. 2.3 as two parabola-shaped curves). The orbits starting ‘outside’ $\mathcal{B}(\mathbf{p}_+)$ (in the dark-gray region) diverge to infinity. Since \mathbf{p}_+ is attracting, its stable set is simply its basin $\mathcal{B}(\mathbf{p}_+)$, and one branch of $W^u(\mathbf{p}_-)$ clearly tends to \mathbf{p}_+ with $t \rightarrow \infty$ (the other branch diverges to infinity). The unstable set is $W^u(\mathbf{p}_+) = \emptyset$, because $H_{a,b}$ is invertible.

2.4 Homoclinic Bifurcations

In this section we explain such notions as a homoclinic orbit and a homoclinic bifurcation. A homoclinic orbit is often a basic tool for rigorously showing existence of chaotic dynamics [10, 33]. In spaces with dimension greater than one, a homoclinic bifurcation is related to a homoclinic tangle. The latter represents a structure where stable and unstable sets of a saddle fixed point twist and interlace in a very complex manner. Whenever this intersection is transverse, there exists an invariant set on which the restriction of the map is chaotic.

As for a one-dimensional DDS, there is no concept of a saddle point. However, if the map is noninvertible, the stable set of a repelling fixed point may be nonempty (as was mentioned above). Then, homoclinic bifurcations are also possible but the

scenario is slightly different from the one involving a saddle point. Namely, the homoclinic orbit has to be mapped directly to a repelling fixed point after a finite number of iterates. Moreover, homoclinic orbits of this kind also appear in noninvertible higher-dimensional maps. As was proved by Marotto [22], a non-degenerate homoclinic orbit of an expanding fixed point (a snap-back repeller) is associated with an invariant set on which the map is chaotic.

2.4.1 The Notion of a Homoclinic Orbit

In simple words, a homoclinic orbit is the one that tends to the same invariant set in both the forward and the backward processes. Whenever the stable and unstable sets of a fixed point intersect, this induces such a homoclinic orbit. We give all definitions for fixed points and remark that to get similar definitions for k -cycles it is enough to consider the k -th iterate of the map T^k .

Definition 2.5 Let \mathbf{x}^* be a hyperbolic fixed point of a map T . Any point $\mathbf{y} \in W^s(\mathbf{x}^*) \cap W^u(\mathbf{x}^*) \setminus \{\mathbf{x}^*\}$ is called *homoclinic*.

If a homoclinic point exists, then infinitely many homoclinic points must also exist, accumulating in a neighborhood of \mathbf{x}^* . Intuitively, this can be understood by observing that the images of \mathbf{y} and its suitable preimages are also homoclinic points, which converge to \mathbf{x}^* .

Definition 2.6 A sequence of images and suitable preimages of a homoclinic point \mathbf{y} , which converge to \mathbf{x}^* , is called a *homoclinic orbit* of \mathbf{x}^* .

In other words, a homoclinic orbit is an infinite set of points

$$\mathcal{O}_h(\mathbf{x}^*) = \{\dots, \mathbf{y}_{-t}, \dots, \mathbf{y}_{-1}, \mathbf{y}_0, \mathbf{y}_1, \dots, \mathbf{y}_t, \dots\} \quad (2.13)$$

such that $T^t(\mathbf{y}_{-t}) = \mathbf{y}_0$ and $\mathbf{y}_t = T^t(\mathbf{y}_0)$ with

$$\lim_{t \rightarrow \infty} \mathbf{y}_{-t} = \mathbf{x}^*, \quad \lim_{t \rightarrow \infty} \mathbf{y}_t = \mathbf{x}^*.$$

It is sometimes important to distinguish between critical and noncritical homoclinic orbits. A homoclinic orbit is called *critical* if it contains a critical point, that is, a point at which the map T is not locally invertible. Otherwise, a homoclinic orbit is *noncritical* (see, e.g., [13]). For instance, in case of a unimodal map a homoclinic orbit including the local extremum point is critical.

2.4.2 Homoclinic Orbits for One-Dimensional Maps

By analyzing a simple example we explain how homoclinic orbits appear in scalar maps and what is a homoclinic bifurcation in this case. Consider a famous logistic map $T_\mu(x) = \mu x(1 - x)$, $T_\mu : [0, 1] \rightarrow [0, 1]$. In Fig. 2.4a the bifurcation diagram of T_μ is plotted, where the dashed curve indicates the fixed point $x^* = 1 - 1/\mu$ when it becomes unstable, while the black vertical line corresponds to the parameter value $\mu = \mu^* \approx 3.6786$, at which a homoclinic bifurcation occurs. The graphs of T_μ with $\mu < \mu^*$, $\mu = \mu^*$, and $\mu > \mu^*$ appear in Fig. 2.4b, c and d, respectively. A few steps of the forward orbit of the extremum point $x_e = 1/2$ are also plotted.

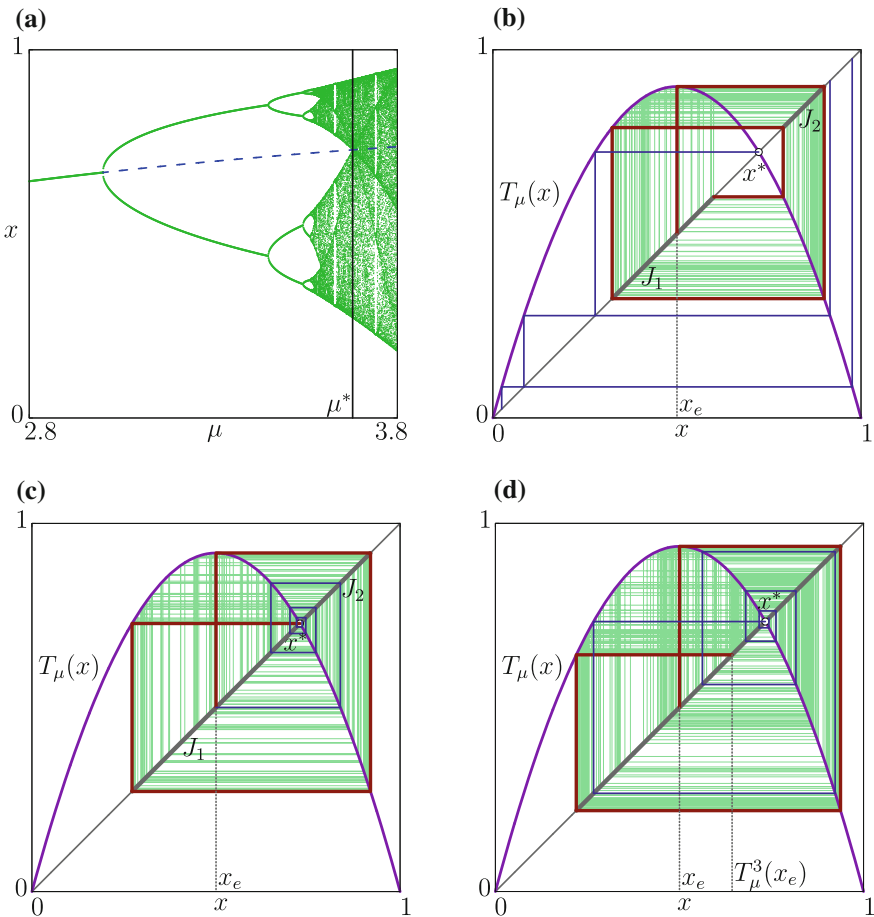


Fig. 2.4 Logistic map: A bifurcation diagram in (a); and the map dynamics (b) before, c at, and d after the first homoclinic bifurcation of the fixed point x^*

As can be noticed in Fig. 2.4b, typical asymptotic orbits of T_μ (see the shown staircase diagram) never exit intervals $J_1 \cup J_2$ which are bounded by the first four images of the extremum point x_e . Note that $T_\mu^3(x_e)$ is greater than x^* . As for the fixed point x^* , the set of all its preimages can be divided into two sequences. The first (left) sequence approaches zero with increasing rank. The second (right) sequence consists of points which do not have preimages. This implies that x^* cannot have homoclinic orbits.

In Fig. 2.4c the point x_e is clearly homoclinic. On one hand, in three steps x_e is mapped into x^* , that is, $T^3(x_e) = x^*$. On the other hand, there exists an appropriate backward orbit of x_e that tends to x^* , since the fixed point is repelling. This moment corresponds to the first homoclinic bifurcation of x^* . Due to the equality $T^3(x_e) = x^*$, the two intervals J_1 and J_2 merge at x^* creating a single invariant interval J , which persists after the bifurcation.

For $\mu > \mu^*$ (see Fig. 2.4d) the image $T_\mu^3(x_e)$ is less than x^* (in contrast to the case before the bifurcation where it was greater than x^*). Then, there exists a sequence of preimages of x^* that tends to x^* with increasing rank, thus, constituting a homoclinic orbit of x^* (dotted line). This implies that there exists a subset $\Lambda \subset J$ such that the restriction $T_\mu|_\Lambda$ is chaotic in sense of Devaney.

The mechanism of homoclinic bifurcation described above is common for a class of unimodal maps with a local maximum or minimum. We formulate the following theorem for maps with a local maximum, which can be easily modified to get similar statement for maps with local minimum.

Theorem 2.2 *Let $T : I \rightarrow I$ be a unimodal continuous map of the interval $I \subset \mathbb{R}$ into itself and denote the point of maximum of T as x_e . Suppose that*

1. T is smooth in $I \setminus \{x_e\}$;
2. T has a unique unstable fixed point x^* ;
3. there exists a sequence of preimages of x_e approaching x^* .

Then when $T^3(x_e) = x^$, there occurs a (critical) homoclinic orbit of the fixed point x^* . Furthermore, for $T^3(x_e) < x^*$ there exists a closed invariant set $\Lambda \subseteq [T^2(x_e), T(x_e)] \subseteq I$ such that the restriction $T|_\Lambda$ is chaotic in sense of Devaney.*

A similar result can be clearly obtained for a k -cycle $\mathcal{C}_k = \{\mathbf{x}_1^*, \dots, \mathbf{x}_k^*\}$ by applying Theorem 2.2 to \mathbf{x}_j^* as fixed points of T^k on suitable intervals I_j . The latter correspond to cyclical intervals of T , that is $T(I_j) = I_{j+1}$, $j < k$, $T(I_k) = I_1$.

Theorem 2.2 can be also used when studying models with “backward dynamics”. That is, the models where the iterative relation is given as $x_t = T(x_{t+1})$, but one is still interested in the behavior of the forward values of the state variable $(x_t, x_{t+1}, x_{t+2}, \dots)$ [11]. Among economic examples there may be mentioned the overlapping generations (OLG) model [14] and the cash-in-advance model [23].

2.4.3 Homoclinic Tangles

In this section we turn to saddle points in dynamical systems of dimension greater than one and their homoclinic orbits. A homoclinic orbit causes the stable and unstable sets of a saddle point \mathbf{x}^* fold, twist and intersect in a rather complex way. Due to its complexity, this structure is referred to as a *homoclinic tangle* (see, e.g., [1, 17]) and often the mechanism of its appearance is as follows. First, a homoclinic tangency between stable $W^s(\mathbf{x}^*)$ and unstable $W^u(\mathbf{x}^*)$ sets occurs. Then tangency turns to transverse crossing that persists for a certain parameter range. Finally, the homoclinic tangle is destroyed through the second tangency between the same branches of $W^s(\mathbf{x}^*)$ and $W^u(\mathbf{x}^*)$ (see Fig. 2.5a–c). Moreover, whenever $W^s(\mathbf{x}^*)$ and $W^u(\mathbf{x}^*)$ intersect transversely, there exists an invariant set Λ such that the restriction of the map to Λ is chaotic (see, e.g., [17, 34]).

Note that asymptotic behavior of the related branches of $W^s(\mathbf{x}^*)$ and $W^u(\mathbf{x}^*)$ differ before and after the homoclinic tangle. Namely, if before the first tangency the suitable branch of $W^s(\mathbf{x}^*)$ tends towards some invariant set A_1 , then after the second tangency this branch must tend towards another invariant set A_2 . The same is true for $W^u(\mathbf{x}^*)$, i.e., it must come from different invariant sets B_1 and B_2 before and after the tangle. Knowing this, one can discover existence of a homoclinic tangle studying asymptotic behavior of stable and unstable sets of a fixed point.

The phenomena described above can be clearly generalized to a saddle k -cycle $\mathcal{C}_k = \{\mathbf{x}_1^*, \dots, \mathbf{x}_k^*\}$ by considering k -th iterate T^k . However, since there are k saddle fixed points for T^k , there are two situations possible. The first situation is complete analogue of what happens for a single fixed point when the stable and unstable sets of *the same* point of the cycle intersect. Namely, $W^s(\mathbf{x}_i^*) \cap W^u(\mathbf{x}_i^*) \neq \emptyset$, $1 \leq i \leq k$. The second situation is when the stable set of each \mathbf{x}_i^* intersects the unstable set of *the next* point \mathbf{x}_{i+1}^* (we assume $i + 1 = 1$ for $i = k$), that is, $W^s(\mathbf{x}_i^*) \cap W^u(\mathbf{x}_{i+1}^*) \neq \emptyset$. In this case, it is sometimes said that there exist *heteroclinic orbits* for points \mathbf{x}_i^* , $1 \leq i \leq k$, and the structure of their stable and unstable sets is referred to as a *heteroclinic tangle*.

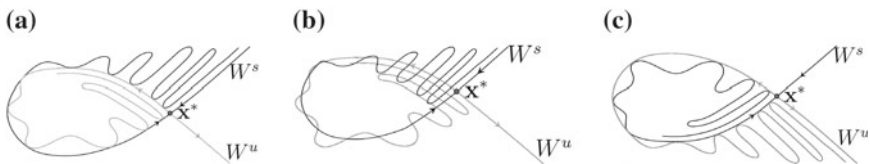


Fig. 2.5 A homoclinic tangle: **a** the first homoclinic tangency; **b** transverse intersection of the stable and unstable manifolds; **c** the second homoclinic tangency

2.4.4 Homoclinic Orbits in 2D: Smale Horseshoe

In two-dimensional systems, a prototypical example for chaotic behavior related to homoclinic orbits of saddle points is a *Smale horseshoe*. Thorough understanding of asymptotic behavior related to this structure is essential for understanding certain aspects of global dynamics of specific real systems. The map possessing the Smale horseshoe was introduced by Smale [33] while studying dynamics of orbits of the van der Pohl oscillator. The action of the map is defined geometrically by squeezing the square, then stretching the result into a long strip, and, finally, folding the strip into the shape of a horseshoe as shown in Fig. 2.6 (see also [3, 7, 34]).

More formally, let us consider a region Δ consisting of three components: a central square Q with side length 1 and two semidisks D_1 and D_2 at either end (that is, Δ is shaped like a “stadium”). The horseshoe map F takes Δ inside itself according to the following prescription. First, F linearly contracts Q in the vertical direction by a factor $\delta < 1/2$, while the regions D_1 and D_2 are contracted so as to remain semidisks attached to the resulting rectangle. Then, F expands Q in the horizontal direction by a factor $1/\delta$ so that it is long and thin (D_1 and D_2 remain unchanged). Finally, F puts Q back inside Δ in a horseshoe-shaped figure. The regions D_1 and D_2 are then mapped into D_1 . We remark that $F(\Delta) \subset \Delta$ and that F is one-to-one, however, since F is not onto, the inverse F^{-1} is not globally defined. In particular, only the points belonging to the two horizontal stripes shaded in Fig. 2.6 has rank-1 preimages in the square Q .

Figure 2.7 serve to clarify this point, where only the region Q is shown for compactness. The two stripes which has rank-1 preimages are denoted H_0 and H_1 and both has height δ . The preimages of H_0 and H_1 constitute two vertical stripes V_0 and V_1 (both of the width δ) also shown in Fig. 2.7a. For sake of simplicity, we assume that V_0 and V_1 are mapped linearly onto H_0 and H_1 . This assumption implies that F preserves horizontal and vertical lines in Q . For later use we note the following property of F .

LP Let $\ell_h \subset Q$ be a horizontal line segment of length a , such that $F(\ell_h) \subset Q$. Then, $F(\ell_h)$ is also a horizontal line segment whose length is a/δ . Similarly, let $\ell_v \subset Q$, $F(\ell_v) \subset Q$, be a vertical line segment of length b , then, $F(\ell_v)$ is also a vertical line segment whose length is $b\delta$.

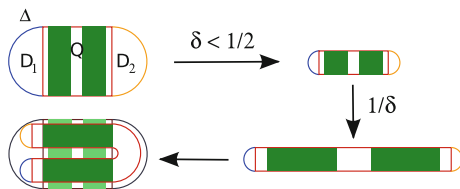


Fig. 2.6 Schematic (geometric) representation of one iterate of a horseshoe map

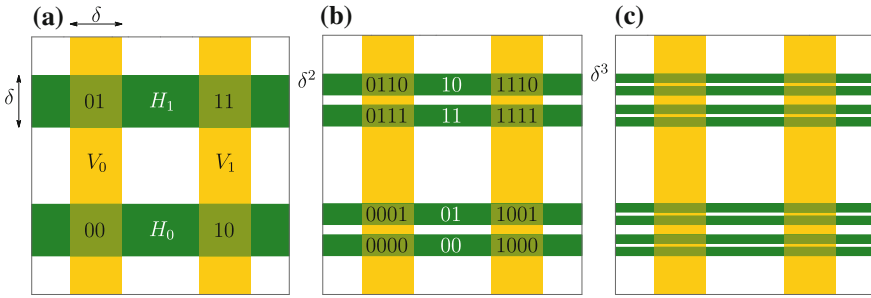


Fig. 2.7 Consecutive construction of images of the square Q under action of the Smale horseshoe map F . **a** The first image $F(Q) \cap Q$ consists of two horizontal stripes H_0 and H_1 of height δ . **b** The second image $F^2(Q) \cap Q$ is represented by four stripes of height δ^2 . **c** The third image $F^3(Q) \cap Q$ is eight δ^3 -height stripes

In other words, F preserves vertical and horizontal line segments belonging to Q if they are mapped into Q .

Now, we turn to describing asymptotic dynamics of orbits of F . First, note that F is a contraction in D_1 , hence, there is a unique attracting fixed point $\mathbf{p} \in D_1$, that is, $\lim_{t \rightarrow \infty} F^t(\mathbf{y}) = \mathbf{p}$ for any $\mathbf{y} \in D_1$. Since $F(D_2) \subset D_1$, all forward orbits in D_2 behave likewise. Similarly, if $\mathbf{y} \in Q$ but $F^t(\mathbf{y}) \notin Q$ for some $t > 0$, then we must have $F^t(\mathbf{y}) \in D_1 \cup D_2$, so that the orbit $\mathcal{O}(\mathbf{y})$ also converges to \mathbf{p} . Consequently, to understand the forward orbits of F , it suffices to consider the set of points whose forward orbits lie for all time in Q , that is,

$$\Lambda = \{\mathbf{y} \in Q : F^t(\mathbf{y}) \in Q, t \geq 0\} = \bigcap_{t=-\infty}^{\infty} F^t(Q). \tag{2.14}$$

It can be shown, that most points eventually leave the square Q under the action of F , and the remaining invariant set Λ is a Cantor set. Recall that a *Cantor set* is an uncountable set with no connected subsets (except individual points). In a space of dimension greater than one such a set is sometimes referred to as a *Cantor dust*.

Construction of the invariant set Λ is an inductive process, and it is convenient to construct separately those parts corresponding to forward iterates and backward iterates, taking further their intersection to obtain Λ . As it has been already said, $Q_1 = Q \cap F(Q) = H_0 \cup H_1$. Since only points belonging to $V_0 \cup V_1$ stay in Q under F , only the points belonging to the intersection of H_0, H_1 and V_0, V_1 are mapped into Q under next iteration of F . In Fig. 2.7a these four squares are marked by symbols 00, 01, 10, and 11. The image $Q_2 = F(Q_1) \cap Q = F^2(Q) \cap F(Q) \cap Q$ (of the squares 00, 01, 10, and 11) is made up of four horizontal stripes as in Fig. 2.7b (each stripe is of height δ^2). Similarly, only the points belonging to the intersection of Q_2 and V_0, V_1 are mapped into Q under F generating $Q_3 = F(Q_2) \cap Q = F^3(Q) \cap F^2(Q) \cap F(Q) \cap Q$, which is constituted by eight horizontal stripes of height δ^3 (see Fig. 2.7c). Inductively, the set $Q^t = \bigcap_{j=0}^t F^j(Q)$, $F^0(Q) = Q$, consists of 2^t horizontal stripes

each having width δ^t . Thus, the part of Λ corresponding to forward iterates of F denoted

$$\Lambda_+ = \cap_{t=0}^{\infty} F^t(Q)$$

is the product of a Cantor set with a horizontal interval.

By similar arguments it is easy to check that the rank- t preimage of Q which is contained in Q consists of 2^t vertical stripes of the width δ^t . Hence, the part of Λ corresponding to backward iterates

$$\Lambda_- = \cap_{t=-\infty}^0 F^t(Q)$$

is the product of a Cantor set with a vertical interval. This implies that the invariant set $\Lambda = \Lambda_+ \cap \Lambda_-$ is also a Cantor set (a two-dimensional Cantor dust). In Fig. 2.8 the first three approximations of Λ are shown.

It is possible to show further, that this invariant Cantor set Λ is in one-to-one correspondence with the set Σ_2 of bi-infinite binary sequences. Recall that Σ_2 is defined as

$$\Sigma_2 = \{(s) = (\dots s_{-2}s_{-1} \cdot s_0s_1s_2 \dots) : s_j = 0 \text{ or } 1\}$$

with the metric $d((s), (t)) = \sum_{i=-\infty}^{\infty} 2^{-|i|} |s_i - t_i|$. Introduce also the *shift* map σ as

$$\sigma(\dots s_{-2}s_{-1} \cdot s_0s_1s_2 \dots) = (\dots s_{-2}s_{-1}s_0 \cdot s_1s_2 \dots),$$

which is known to be chaotic. It can be proved that the restriction $F|_{\Lambda}$ is topologically conjugate to σ , which proves that $F|_{\Lambda} : \Lambda \rightarrow \Lambda$ is chaotic as well (see, e.g., [7]).

What has that got to do with homoclinic orbits? one may ask. Indeed, above we have mentioned only one fixed point $\mathbf{p} \in D_1$ which is attracting, and hence any point in Q which eventually leaves Q belongs to the stable set of \mathbf{p} . However, the map F has two more fixed points belonging to Λ which are saddles (their existence can be proved by using symbolic sequences of zeros and ones, for more detail see

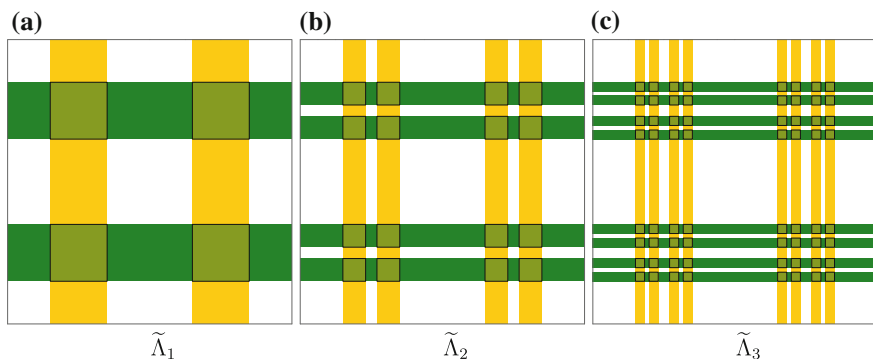
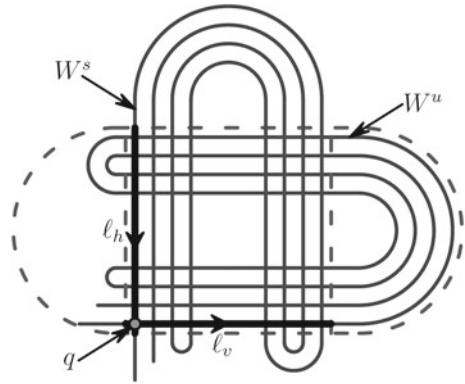


Fig. 2.8 First three approximations of the invariant Cantor set Λ

Fig. 2.9 Transverse homoclinic intersection of the stable W^s and unstable W^u sets of a saddle fixed point q for a horseshoe map



[7, 34]). The stable and unstable sets of these points have much more complex structure. For example, consider a fixed point $\mathbf{q} \in V_0 \cap H_0 \subset Q$. Figure 2.9 shows \mathbf{q} together with $W^s(\mathbf{q})$ and $W^u(\mathbf{q})$, which clearly mimic the “fold-and-pleat” behavior of F . Any point that lies on the vertical segment ℓ_v through \mathbf{q} belongs to $W^s(\mathbf{q})$. Indeed, since at each iteration of F the segment ℓ_v is squeezed by factor δ , the points from ℓ_v constantly approach \mathbf{q} . Clearly, all preimages $F^{-t}(\ell_v)$, $t \geq 1$, belong to $W^s(\mathbf{q})$ as well. Due to property LP these preimages constitute a set of vertical segments of length 1. More precisely, $F^{-t}(\ell_v)$ consists of 2^t such segments. Similarly, the horizontal segment ℓ_h through \mathbf{q} belongs to $W^u(\mathbf{q})$, as well as all its forward images $F^t(\ell_h)$. It can be checked, that $F^t(\ell_h) \subset \Delta$ is a “snake-like” curve that cuts across Q exactly 2^t times. This inevitably implies that $W^s(\mathbf{q}) \cap W^u(\mathbf{q}) \neq \emptyset$, and, hence, there exists infinite number of points which are homoclinic to \mathbf{q} .

Let us show that as soon as for an invertible map T there exists a transverse homoclinic orbit (that is, the stable and the unstable sets intersect transversally), then there also exists a related horseshoe-like structure. We start with a rectangle R containing a fixed point \mathbf{x}^* of the map T . Successive iterates of T stretch R out along the unstable set $W^u(\mathbf{x}^*)$. Under iterates of T^{-1} , it is stretched out along the stable set $W^s(\mathbf{x}^*)$. In particular, there exist numbers l and k such that $T^{-l}(R)$ extends along the stable set to include some homoclinic point \mathbf{y} , and $T^k(R)$ extends along the unstable set to include \mathbf{y} as well (see Fig. 2.10). Thus T^{k+l} is a horseshoe map with the “square” domain $Q = T^{-l}(R)$ and its image $T^k(R)$. This can be summarized as

Theorem 2.3 [33] *Let T be a diffeomorphism of the plane, and let \mathbf{x}^* be a saddle fixed point. If the stable and unstable manifolds of \mathbf{x}^* cross transversally, then there is a hyperbolic horseshoe for some iterate of T .*

Note that in order to have exactly the dynamics of the ideal horseshoe, there must be uniform stretching and contraction at points in the invariant set, which is unlikely to happen in a real system. Thus, the domains which are squares and rectangles for the pure horseshoe map in real systems are somewhat deformed (though being still topologically conjugate to “ideal” shapes).

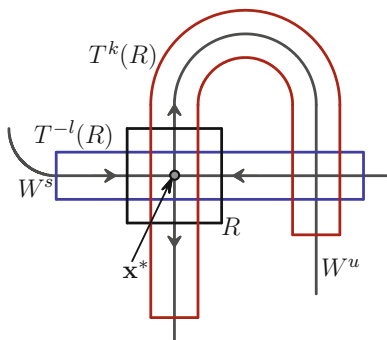


Fig. 2.10 A horseshoe generated from a homoclinic orbit. The domain $T^{-l}(R)$ corresponds to the square Q , while the domain $T^k(R)$ is its *horseshoe-shape* image. The iterate T^{k+l} is a horseshoe map

Example 2.6 Theorem 2.3 guarantees that presence of a transverse homoclinic point implies chaotic orbits (although we cannot say anything about whether they are attracting or not). Let us illustrate this by an example. We consider the Hénon map $H_{a,b}$ defined in (2.11) with $a = 2.1, b = 0.3$. Figure 2.11a (cf. Fig. 2.10) shows the stable and the unstable sets of the saddle point $\mathbf{p}_+ = (x_+, x_+)$ which is marked by a circle. The initial area \tilde{R} is not a rectangle but a parallelepiped snapped onto the related eigenvectors. The rank-4 image $R_4 = H_{a,b}^4(\tilde{R})$ of \tilde{R} and its rank-2 preimage $R_{-2} = H_{a,b}^{-2}(\tilde{R})$ are also shown. Figure 2.11b is a zoomed window marked by letter ‘b’ in Fig. 2.11a, in which one can clearly see that the intersection $R_4 \cap R_{-2} \neq \emptyset$. Hence, $H_{a,b}^6$ is topologically conjugate to the Smale horseshoe.

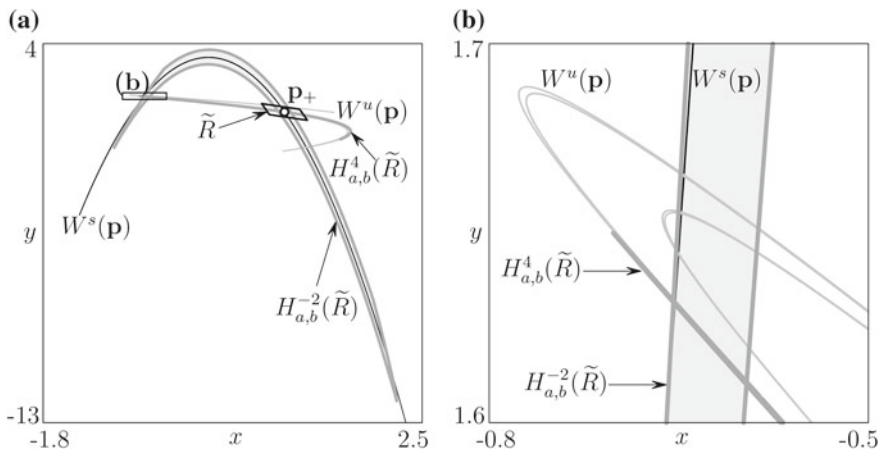


Fig. 2.11 Horseshoe structure in the Hénon map. Plot **b** is a zoom of the *rectangle* marked ‘b’ in **a**

2.5 Crises

In this section we describe bifurcations which concern transformation or disappearance of chaotic attractors. Chaotic attractors are unlike fixed points or cycles not only because they are infinite sets. A periodic point can not abruptly change its periodicity or location while existent. With varying parameters it can only change its stability characteristics or disappear through the related bifurcation. On the contrary, a chaotic attractor may undergo sudden dramatic transformation under small variations of the map parameters. Such sharp changes are called *crises* and can include sudden appearance or disappearance of the attractor or a discontinuous variation in its size or shape [3, 16, 27]. Very commonly, these transformations occur when a chaotic attractor has a contact with some unstable invariant set (e.g., the stable set of a saddle periodic point).

2.5.1 Interior Crisis

Interior crisis is a bifurcation due to which a chaotic attractor \mathcal{Q} experiences a sudden change in size and shape. In simple words, this phenomenon can be explained as follows. Let \mathbf{x}^* be an unstable periodic point with nonempty stable $W^s(\mathbf{x}^*)$ and unstable $W^u(\mathbf{x}^*)$ sets, which belongs to the interior of the basin of \mathcal{Q} . At some critical (bifurcation) parameter value the attractor \mathcal{Q} has a contact with \mathbf{x}^* (or, equivalently, with $W^s(\mathbf{x}^*)$). After the bifurcation the point \mathbf{x}^* joins \mathcal{Q} which implies the whole unstable set $W^u(\mathbf{x}^*)$ to be “swallowed up” by \mathcal{Q} as well. This clearly leads to swift transformation of \mathcal{Q} .

To explain this in more detail, we analyze a simple example. Let consider Ikeda map family $g : \mathbb{R}^2 \rightarrow \mathbb{R}^2$ given by

$$g : \begin{pmatrix} x \\ y \end{pmatrix} \mapsto \begin{pmatrix} A + bx \cos(m) - by \sin(m) \\ by \cos(m) + bx \sin(m) \end{pmatrix} \quad (2.15)$$

with

$$m = \phi - \frac{q}{1 + x^2 + y^2}. \quad (2.16)$$

The system having more general form was proposed first by Ikeda [19] as a model of light going around across a nonlinear optical resonator. In [20] the original map was reduced to the simplified form given above.

We fix all the parameters except q . Figure 2.12a, b show the chaotic attractor \mathcal{Q}_q of g for two different parameter values: before ($q = 7.1$) and after ($q = 7.3$) the crisis. There are two different attractors here: (i) the sink fixed point \mathbf{p} whose basin is the shaded area and (ii) the chaotic attractor \mathcal{Q}_q whose basin is shown white. The two basins are separated by the stable set of the saddle fixed point \mathbf{q} .

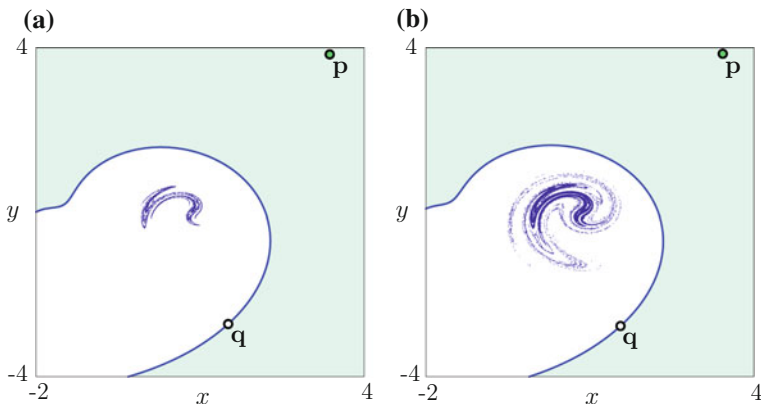


Fig. 2.12 State space of the Ikeda map with $A = 0.84, b = 0.9, \phi = 0.4$ and **a** $q = 7.1 < q_c$, **b** $q = 7.3 > q_c$. The basins of the stable fixed point \mathbf{p} and the chaotic attractor \mathcal{Q}_q are separated by the stable set of the saddle point \mathbf{q}

Simple numerical experiments for intermediate values of q (between 7.1 and 7.3) show that the shape of \mathcal{Q}_q varies only slightly from that shown in Fig. 2.12a for $7.1 < q \leq q_c \approx 7.24$. For $q > q_c$, however, the attractor in this region of the plane suddenly becomes much larger. So that, the attractor does not continuously increase in size as q passes q_c , as it happens in local bifurcations for periodic points.

Let us discover what happens at a crisis value q_c . It appears that for all q being close to q_c there exist a saddle 5-cycle \mathcal{C}_5 in the vicinity of \mathcal{Q}_q (in fact, there exist several 5-cycles, but only one is relevant to the phenomenon investigated). For $q < q_c$ the cycle \mathcal{C}_5 does not belong to the attractor \mathcal{Q}_q . As q approaches q_c from below, the distance between \mathcal{Q}_q and \mathcal{C}_5 (equivalently, $W^s(\mathcal{C}_5)$) goes to zero. At $q = q_c$ the attractor \mathcal{Q}_q and the cycle \mathcal{C}_5 ($W^s(\mathcal{C}_5)$) collide. Then, after the crisis the chaotic attractor \mathcal{Q}_q absorbs \mathcal{C}_5 together with its unstable set $W^u(\mathcal{C}_5)$. The result of such crossing between chaotic attractor and the stable set of some periodic point can be formalized as follows (see, e.g., [3]).

Lemma 2.1 (Lambda or Inclination Lemma) *Let T be a diffeomorphism of the plane, and let \mathbf{x}^* be a hyperbolic saddle fixed point of T . Suppose that a curve L crosses the stable manifold $W^s(\mathbf{x}^*)$ transversally. Then each point in the unstable manifold $W^u(\mathbf{x}^*)$ is a limit point of $\cup_{t>0} T^t(L)$.*

The proof of Lemma 2.1 can be found, e.g., in [28].

In other words, if a curve L crosses the stable manifold $W^s(\mathbf{x}^*)$ transversally, then forward iterates of L limit on the entire unstable manifold $W^u(\mathbf{x}^*)$ (see Fig. 2.13). Specifically, it means that for each point $\mathbf{y} \in W^u(\mathbf{x}^*)$ and for any ε -neighborhood $U_\varepsilon(\mathbf{y})$, there exists $t > 0$ such that $T^t(L) \cap U_\varepsilon(\mathbf{y}) \neq \emptyset$. Similar property is known to be true also for noninvertible maps, but there is no rigorous proof for general case.

Using Lemma 2.1, we can interpret the crisis in the Ikeda example above. Figure 2.14a shows that as a parameter q comes close to a critical value q_c , the

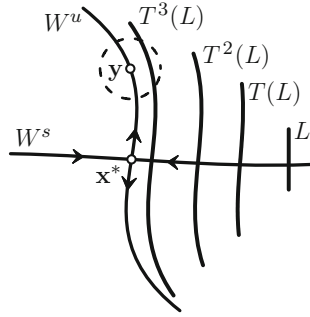


Fig. 2.13 Whenever a curve L crosses the stable set of a saddle \mathbf{x}^* transversally, forward iterates of L approach the unstable set of \mathbf{x}^*

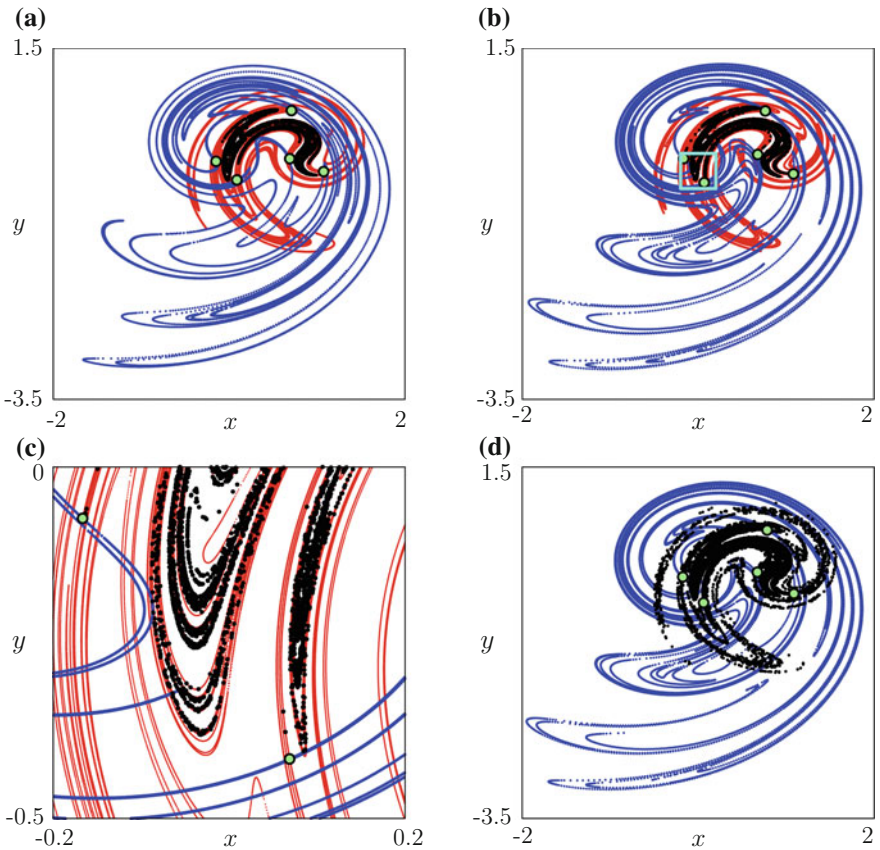


Fig. 2.14 Interior crisis for the chaotic attractor \mathcal{Q}_q of the Ikeda map. **a** Before the crisis, $q = 7.1$; **b** at the crisis value $q = q_c \approx 7.24$; **c** zoom of box outlined *light-blue* in **(b)**; **d** after the crisis $q = 7.3$. *Green points* mark the saddle 5-cycle \mathcal{C}_5 , whose stable and unstable sets are shown by *blue* and *red* lines, respectively. The other parameters are $A = 0.84$, $b = 0.9$, $\phi = 0.4$

attractor \mathcal{Q}_q approaches the stable set $W^s(\mathcal{C}_5)$. At q_c the outer edge of \mathcal{Q}_{q_c} is tangent to this stable set, as shown in Fig. 2.14b (see also Fig. 2.14c which is a zoom of the rectangle indicated in Fig. 2.14b). Finally, for $q > q_c$ the attractor has crossed the stable set $W^s(\mathcal{C}_5)$ (Fig. 2.14d). Once there is a crossing, Lemma 2.1 tells us that forward iterates of portions of \mathcal{Q}_q limit on the entire unstable set $W^u(\mathcal{C}_5)$. Consequently, for $q > q_c$ the attractor \mathcal{Q}_q contains $W^u(\mathcal{C}_5)$. In simple words, having a contact with the stable set of the saddle cycle \mathcal{C}_5 , the chaotic attractor \mathcal{Q}_q absorbs this cycle, but it inevitably follows that \mathcal{Q}_q also absorbs the unstable set of this cycle. It is important that $W^u(\mathcal{C}_5)$ is contained in the basin of attraction of \mathcal{Q}_q for q near q_c . In this case it is said that there is an *interior crisis* at $q = q_c$, and sudden increase of the attractor size is a specific feature of such crises.

Note that the structure of the “smaller” attractor (which is relevant for $q < q_c$) is still apparent in Fig. 2.14d for $q > q_c$. It appears darker since orbits spend a larger percentage of iterates in this region. The closer $q > q_c$ is to the crisis parameter value q_c , the longer orbits typically stay on the “former” attractor before following the new larger structure (cf. Fig. 2.12b).

2.5.2 Boundary Crises

We have considered above the situation when a chaotic attractor \mathcal{Q} contacts the stable set of a saddle periodic point belonging to the interior of the basin $\mathcal{B}(\mathcal{Q})$. It may, however, happen that a saddle point \mathbf{x}^* is on the *boundary* of $\mathcal{B}(\mathcal{Q})$ before the bifurcation (recall that in invertible maps basin boundaries are often consisted of stable sets of saddle points). Then, it is said that at the moment of contact between \mathcal{Q} and $W^s(\mathbf{x}^*)$ there occurs a *boundary crisis*. In this case there are points in $W^u(\mathbf{x}^*)$ which go to another attractor (perhaps infinity). Then for the parameter value greater than the critical value, the chaotic attractor \mathcal{Q} (as well as its basin) no longer exists. However, if a parameter exceeds the critical value only slightly, typical orbits spend many iterates on the “former” chaotic attractor before escaping from its neighborhood. This behavior is called *transient chaos*, and the transient structure itself is called a “ghost” of the chaotic attractor \mathcal{Q} .

We illustrate this again by using the Ikeda map family (2.15) with $b = 0.9$, $\phi = 0.4$, $q = 6$ and changing A through $A_c \approx 1$. For $A < A_c$, the stable set of the saddle fixed point \mathbf{q} forms the boundary between the basins of the sink fixed point \mathbf{p} and the chaotic attractor \mathcal{Q}_A . In Fig. 2.15a it can be seen that one branch of $W^u(\mathbf{q})$ goes to \mathcal{Q}_A , and the other branch goes to \mathbf{p} . For $A = A_c$ the attractor \mathcal{Q}_{A_c} collides with the boundary of its basin (that is, $W^s(\mathbf{q})$), and for $A > A_c$ it no longer exists (and all points from the former basin of \mathcal{Q}_A approach \mathbf{p}). However, as shown in Fig. 2.15b, some orbits spend many iterates on what was the structure of \mathcal{Q}_A before crossing the stable set $W^s(\mathbf{q})$ and converging to \mathbf{p} .

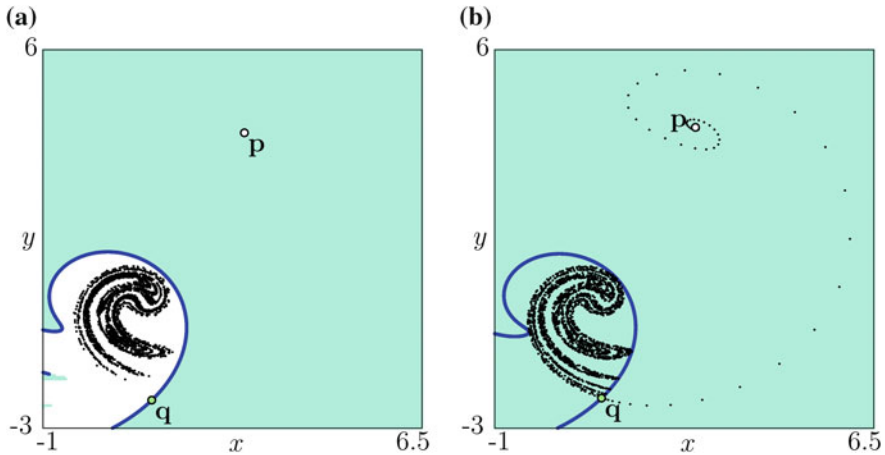


Fig. 2.15 Boundary crisis for the chaotic attractor \mathcal{Q}_A of the Ikeda map. **a** Before the crisis, $A = 0.95$, the stable set of the saddle fixed point \mathbf{q} separates the two basins, $\mathcal{B}(\mathcal{Q}_A)$ and $\mathcal{B}(\mathbf{p})$. **b** After the crisis, $A = 1.003$, there is a “ghost” attractor. Other parameters are $b = 0.9$, $\phi = 0.4$, $q = 6$

2.6 Conclusions

Dynamical systems theory distinguishes two types of bifurcations: those which can be studied in a small neighborhood of an invariant set (local) and those which cannot (global). In this chapter we focused on several aspects of global bifurcation analysis of discrete time dynamical systems, such as homoclinic bifurcations and crises. There are also other global phenomena being important when investigating a dynamical system. Among them there are bifurcations related to appearance of closed invariant curves and those which cause qualitative changes in the basin structure (for example, when a connected basin becomes nonconnected). For further reading and deeper understanding of all these aspects, we may suggest [1, 24, 25] and references therein.

References

1. Agliari, A., Bischi, G.I., Dieci, R., Gardini, L.: Global bifurcations of closed invariant curves in two-dimensional maps: a computer assisted study. *Int. J. Bifurcat. Chaos* **15**(4), 1285–1328 (2005)
2. Agliari, A., Gardini, L., Puu, T.: Some global bifurcations related to the appearance of closed invariant curves. *Math. Comput. Simul.* **68**, 201–219 (2005)
3. Alligood, K.T., Sauer, T.D., Yorke, J.A.: *Chaos: An Introduction to Dynamical Systems*. Springer, New York (1996)
4. Banks, J., Brooks, J., Cairns, G., Davis, G., Stacey, P.: On Devaney’s definition of chaos. *Am. Math. Mon.* **99**(4), 332–334 (1992)
5. Bischi, G.I., Gardini, L., Kopel, M.: Analysis of global bifurcations in a market share attraction model. *J. Econ. Dyn. Control* **24**, 855–879 (2000)

6. Brock, W.A., Hommes, C.H.: *Econometrica* **65**(5), 1059–1095 (1997)
7. Devaney, R.L.: *An Introduction to Chaotic Dynamical Systems*. Addison-Wesley, Redwood City (1989)
8. de Vilder, R.: Complicated endogenous business cycles under gross substitutability. *J. Econ. Theory* **71**, 416–442 (1996)
9. Farmer, J.D., Ott, E., Yorke, J.A.: The dimension of chaotic attractors. *Phys. D* **7**(1–3), 153–180 (1983)
10. Gardini, L.: Homoclinic bifurcations in n -dimensional endomorphisms, due to expanding periodic points. *Nonlinear Anal.: Theory Methods Appl.* **23**(8), 1039–1089 (1994)
11. Gardini, L., Hommes, C.H., Tramontana, F., de Vilder, R.: Forward and backward dynamics in implicitly defined overlapping generations models. *J. Econ. Behav. Organ.* **71**, 110–129 (2009)
12. Gardini, L., Mira, C.: Noninvertible maps. In: *Nonlinear Economic Dynamics*, pp. 239–254. Nova Science Publishers, Inc. (2010)
13. Gardini, L., Sushko, I., Avrutin, V., Schanz, M.: Critical homoclinic orbits lead to snap-back repellers. *Chaos Solitons Fractals* **44**, 433–449 (2011)
14. Grandmont, J.M.: Expectations driven nonlinear business cycles. In: *Rheinisch-Westfälische Akademie der Wissenschaften*. VS Verlag für Sozialwissenschaften (1993)
15. Grebogi, C., Ott, E., Pelikan, S., Yorke, J.A.: Strange attractors that are not chaotic. *Phys. D* **13**, 261–268 (1984)
16. Grebogi, C., Ott, E., Yorke, J.A.: Crises, sudden changes in chaotic attractors, and transient chaos. *Phys. D* **7**(1–3), 181–200 (1983)
17. Guckenheimer, J., Holmes, P.: *Nonlinear oscillations, dynamical systems and bifurcations of vector fields*. Applied Mathematical Sciences, vol. 42. Springer (1983)
18. Hénon, M.: A two-dimensional mapping with a strange attractor. *Commun. Math. Phys.* **50**(1), 69–77 (1976)
19. Ikeda, K.: Multiple-valued stationary state and its instability of the transmitted light by a ring cavity system. *Opt. Commun.* **30**, 257–261 (1979)
20. Ikeda, K., Daido, H., Akimoto, O.: Optical turbulence: chaotic behavior of transmitted light from a ring cavity. *Phys. Rev. Lett.* **45**(9), 709–712 (1980)
21. Li, T.Y., Yorke, J.A.: Period three implies chaos. *Am. Math. Mon.* **82**(10), 985–992 (1975)
22. Marotto, F.R.: Snap-back repellers imply chaos in r^n . *J. Math. Anal. Appl.* **63**(1), 199–223 (1978)
23. Michener, R.W., Ravikumar, B.: Chaotic dynamics in a cash-in-advance economy. *J. Econ. Dyn. Control* **22**, 1117–1137 (1998)
24. Mira, C., Gardini, L.: From the box-within-a-box bifurcations organization to the julia set. Part I. *Int. J. Bifurcat. Chaos* **19**(1), 281–327 (2009)
25. Mira, C., Gardini, L., Barugola, A., Cathala, J.C.: *Chaotic Dynamics in Two-Dimensional Noninvertible Maps*. Nonlinear Science. World Scientific, Singapore (1996)
26. Myrberg, P.J.: Iteration der reellen polynome zweiten grades iii. *Annales Academiæ Scientiarum Fennicæ* **336**, 3–18 (1963)
27. Ott, E.: *Chaos in Dynamical Systems*. Cambridge University Press (1993)
28. Palis, J., de Melo, W.: *Geometric Theory of Dynamical Systems: An Introduction*. Springer, New York (1982)
29. Ruelle, D.P., Takens, F.: On the nature of turbulence. *Commun. Math. Phys.* **20**(3), 167–192 (1971)
30. Sharkovskii, A.N.: Problem of isomorphism of dynamical systems. In: *Proceedings of 5th International Conference on Nonlinear Oscillations*, vol. 2, pp. 541–544 (1969)
31. Sharkovskii, A.N., Maistrenko, Y.L., Romanenko, E.Y.: *Difference Equations and Their Applications*. Kluwer Academic Publisher, Dordrecht (1993)
32. Silverman, S.: On maps with dense orbits and the definition of chaos. *Rocky Mt. J. Math.* **22**(1), 353–375 (1992)
33. Smale, S.: Differentiable dynamical systems. *Bull. Am. Math. Soc.* **73**, 747–817 (1967)
34. Wiggins, S.: *Global Bifurcations and Chaos: Analytical Methods*, Applied Mathematical Sciences, vol. 73. Springer, New York (1988)